

Injection of CO₂-saturated brine in geological reservoir: a way to enhanced storage safety

Nawaz Ahmad^{1,2,*}, Anders Wörman¹, Xavier Sanchez-Vila³, and Jerker Jarsjö⁴, Andrea Bottacin-Busolin⁵ and Helge Hellevang⁶

¹ Department of Civil and Architectural Engineering, KTH Royal Institute of Technology, Brinellvägen 23, 10044, Stockholm, Sweden

² Policy Wing, Ministry of Petroleum and Natural Resources, Islamabad, Pakistan

³ Hydrogeology Group, Department of Geotechnical Engineering and Geosciences, Universitat Politècnica de Catalunya, UPC-BarcelonaTech, 08034 Barcelona, Spain

⁴ Department of Physical Geography and Quaternary Geology, Stockholm University, SE-10691 Stockholm, Sweden

⁵ School of Mechanical, Aerospace and Civil Engineering, University of Manchester, UK

⁶ Department of Geosciences, University of Oslo, Pb. 1047, Blindern, Oslo, Norway 0316.

* Corresponding author Email: nawaza@kth.se

Key Points

- Injection of CO₂-saturated brine to a geological reservoir is modeled
- significant consumption of CO₂ in mineral reactions is observed
- Injection of CO₂-saturated brine may increase the safety of CO₂ geological storage

Abstract: Injection of free phase CO₂ into deep geological reservoirs is associated with risk of considerable return flows towards the land surface due to the buoyancy of CO₂, which is lighter than the resident brine in the reservoir. Such upward movements can be avoided if CO₂ is injected in the dissolved phase. In this work, injection of CO₂-saturated brine in a subsurface carbonate reservoir is modeled. Physical and geochemical interaction of injected low pH brine saturated with CO₂ with the minerals is investigated through reactive transport modeling. Three minerals namely calcite, dolomite, and siderite are included in the reactive transport modeling. CO₂-saturated brine, being low in pH, shows higher reactivity with the reservoir minerals resulting in its significant consumption over the period of time. Over the injection period of 20 years, about 18% of CO₂ injected mass has been consumed in minerals kinetic reactions in various reactive simulation scenarios. Sorption included in the transport analysis resulted in additional quantities of CO₂ mass stored in adsorbed state. However, considered carbonate reservoir was found to offer storage of injected dissolved CO₂ mainly in the form of ionic trapping due to a very small precipitation of carbonate minerals.

Keywords: Injection of CO₂-saturated brine, geological storage reservoir, enhanced mineral trapping, storage safety

1. Introduction

Leakage of CO₂ from storage reservoirs is a main concern related to its geological sequestration [*Haugan and Joos, 2004; Stone et al., 2009; Weir et al., 1996; Kopp et al.,*

2010]. When CO₂ is injected in its supercritical phase (a state between gas and liquid), it is lighter than the resident formation brine and thus has a tendency to move upwards due to buoyancy [Audigane *et al.*, 2007, Xu *et al.*, (2003, 2007); Weir *et al.*, 1996; Garcia, 2001]. Therefore, geological reservoirs overlain by low permeability caprock formations that physically hinder the upward movement of CO₂ are thought to be best candidates for CO₂ storage [García, 2003].

CO₂ is injected as a free-phase in order to sequester the bulk quantities involved but this option is associated with potential leakage risk over the geological time scale. Injected CO₂ stays mainly as a separate free-phase over longer period of time and only small amount is dissolved in the resident brine. CO₂ injected in the reservoir react with *in situ* fluid with its conversion into carbonic acid (solubility trapping-dominates from tens to hundreds of years) followed by conversion into carbon-bearing ionic species (ionic trapping-dominates from hundreds to thousands of years) and then the precipitation of new carbonate minerals resulting in fixation of CO₂ that is the most secure form of sequestration (mineral trapping-dominates over thousands to millions of years) [Metz *et al.*, 2005]. Audigane *et al.*, 2007 has seen only 30% of injected CO₂ converted in dissolved phase after 1000 years and it took 10,000 years to get dissolve all the injected CO₂. They reported only 5% of injected mass consumed in minerals reaction after 10,000 years. Thus if encountered high permeable zones like poorly abandoned wells and fracture or fault zones, CO₂ may leak towards the land surface [Metz *et al.*, 2005, Leonenko and Keith, 2007].

Brine resulting from dissolution of injected CO₂ gets denser than the resident brine and moves downward in the reservoir with reduced leakage risk [Garcia, 2001; Metz *et al.*,

2005; Audigane et al., 2007]. Dissolution of CO₂ in the formation brine also lowers its pH resulting in increased reactivity with the formation minerals [Xu et al., (2003, 2004); Audigane et al., 2007]. Minerals reactions consume CO₂ and thus results in its permanent fixation called as mineral trapping [Audigane et al., 2007]. Minerals dissolution/precipitation caused by geochemical interaction with low pH brine also changes the porosity and permeability of the porous media [Xu et al., (2003)].

Nogues et al., 2013 have conducted numerical study of porosity and permeability evolution at pore scale level driven by inflowing CO₂-saturated water and have suggested that to simplify the geochemical modeling it is appropriate to not include the minerals like kaolinite, anorthite, and albite in cases where carbonate minerals are abundant. Gherardi et al., 2007 have found porosity variations in the vicinity near to reservoir-caprock interface mainly due to calcite mineral reactivity with CO₂ brine. Gaus et al., 2005 has reported decrease in porosity of the caprock as a result of calcite and kaolinite precipitation resulting from dissolution of anorthite over a period of 500 years.

The leakage risk associated with injection of free-phase CO₂ in the subsurface reservoir motivates to inject CO₂ in dissolved phase in order to increase the safety of CO₂ geological storage [Aradottir et al., 2012]. Injection of CO₂ in dissolved phase makes the resulting brine denser (about 1%) than the resident formation brine and thus may tend to move downwards being negatively buoyant after its injection in the reservoir. No cap rock above the reservoir is needed if CO₂ is injected in dissolved form because CO₂-saturated brine is denser than the resident fluids [Sigurdur and Oelkers, 2014]. Also solubility and ionic trapping can take place immediately if CO₂ is injected in dissolved phase in the reservoir [Sigurdur and Oelkers, 2014]. Relatively fast mineral trapping can

also be expected if CO₂ is injected in the dissolved phase [Aradóttir et al., 2012]. CO₂ injected in dissolved phase can only migrate out of the storage reservoir due to regional groundwater movement [Metz et al., 2005]. Subsurface groundwater velocities can be expected on the order of millimetres to centimetres per year [Bachu et al., 1994]. Thus leakage rates of dissolved CO₂ can be expected as substantially lower than for separate-phase CO₂ due to very small groundwater flow velocities in the subsurface [Metz et al., 2005]. Even if the leakage of dissolved CO₂ takes place from the storage reservoir, it will have less potential to reach the land surface due to its very slow movement and its significant retention (stored in pore spaces in dissolved phase, stored in adsorbed state on mineral surfaces and also consumed in geochemical reactions) along the leakage pathway [Ahmad et al, 2014(a,b)(submitted)].

Related to CO₂ geological storage, so far the major focus has been on the injection of CO₂ in supercritical state as a separate-phase in the subsurface reservoir [Matter et al., 2011]. Very few studies have been reported in the literature focusing on the injection of CO₂ in dissolved phase. “CO₂-DISSOLVED” is a research project focussing on injecting CO₂ dissolved in brine. The CarbFix Project aims at injection of CO₂-charged water into the subsurface Basalt rock formation. Various studies have been published in recent years related to The CarbFix Project [for example Matter et al. 2011; Aradóttir et al., 2011; Aradóttir et al., 2012; Tollefson, 2013; Alfredsson et al., 2013; Gislason and Oelkers, 2014]. Aradóttir et al., 2012 have performed reactive transport modeling for injection of dissolved CO₂ in the subsurface basalt rock formation. These authors have injected 40000 tonnes of CO₂ over a period of 10 years in their 2D domain version of simulation using a 100 m vertically thick layer extending up to about 2700 m lying between 400 and 500 m.

However, in their study reactive transport analysis was performed for an extended period of 100 years. These authors have reported about 20% of CO₂ consumed in mineral trapping over the period of 100 years for considered 100 m thick reservoir layer. However, based on storage formation thickness of 400 m, these authors have predicted a consumption of 80% (320000 tonnes consumed out of total 400000 tonnes of injected CO₂).

This study aims at injection of CO₂ in dissolved phase in the subsurface carbonate reservoir thereby including the physical and geochemical interactions with the formation minerals to analyze the amount of CO₂ stored in the aqueous and adsorbed state, amount of CO₂ consumed in geochemical reactions as well as change in porosity and permeability of the reservoir resulting from minerals dissolution and precipitation. In this study we have considered three carbonate rock forming minerals calcite, dolomite, and siderite for geochemical interactions with the injected dissolved CO₂. We have also included the heat exchange between the injected CO₂-saturated brine and the porous media in the reservoir. Results are compared between the various transport scenarios to see the effects of various parameters considered in the study.

2. Numerical modeling technique

Simulations have been performed in COMSOL Multiphysics. Built in user interfaces available in COMSOL Multiphysics are used for coupling all the equations used in the reactive transport modeling. A full coupling between the transport and the chemistry is implemented. Initial and boundary conditions required in the transport modeling are

obtained from the background batch reaction modeling and the CO₂-dissolution modeling. In this study the species Cl⁻ is assumed as conservative at a constant concentration of 0.5mol/kg. As one of the options, CO₂ can be dissolved on the land surface in the brine that is pumped out of the targeted subsurface reservoir and injection of resulting CO₂-saturated brine back in the reservoir [Eke et al., 2011; CO₂-DISSOLVED Project]. However, corrosive nature of brine containing dissolved CO₂ may pose a potential risk of corrosion for the injection pipeline. As an alternate, CO₂ can be transported in a separate line parallel to the one transporting the brine and mixing of these two streams within the injection well before their injection in the subsurface reservoir [Alfredsson et al., 2013; Gislason and Oelkers, 2014].

2.1 Geochemical reactions system

In this study, we have considered three minerals namely calcite, dolomite, and siderite as the rock forming minerals of a synthetic carbonate subsurface reservoir [Zerai, 2006]. Geochemical system to describe the water-rock interaction in the reservoir formation is presented in Table 1.

Table 1: Equilibrium and mineral kinetic reactions considered in this study

No.	Reactions
(R0) ¹	$\text{CO}_{2g} \leftrightarrow \text{CO}_{2aq}$
(R1) ²	$\text{H}_2\text{O} + \text{CO}_{2aq} \leftrightarrow \text{H}^+ + \text{HCO}_3^-$
(R2) ²	$\text{H}_2\text{O} \leftrightarrow \text{H}^+ + \text{OH}^-$
(R3) ²	$\text{HCO}_3^- \leftrightarrow \text{H}^+ + \text{CO}_3^{2-}$

(R4) ²	$\text{Na}^+ + \text{HCO}_3^- \leftrightarrow \text{NaHCO}_{3\text{aq}}$
(R5) ²	$\text{CaHCO}_3^+ \leftrightarrow \text{Ca}^{2+} + \text{HCO}_3^-$
(R6) ²	$\text{MgHCO}_3^+ \leftrightarrow \text{Mg}^{2+} + \text{HCO}_3^-$
(R7) ²	$\text{FeHCO}_3^+ \leftrightarrow \text{Fe}^{2+} + \text{HCO}_3^-$
(R8) ²	$\text{Calcite} + \text{H}^+ \leftrightarrow \text{Ca}^{2+} + \text{HCO}_3^-$
(R9) ²	$\text{Dolomite} + 2\text{H}^+ \leftrightarrow \text{Ca}^{2+} + \text{Mg}^{2+} + 2\text{HCO}_3^-$
(R10) ²	$\text{Siderite} + \text{H}^+ \leftrightarrow \text{Fe}^{2+} + \text{HCO}_3^-$

1. Equilibrium reaction constant is based on *Duan and Sun, 2003* as modified by *Duan et al., 2006*.

2. Equilibrium reaction constants are taken from *The Geochemist's Workbench (GWB)* (default thermodynamic data for the GWB).

Eight reactions (R0 through R7) represent equilibrium reactions whereas rest of the three reactions (R8 through R10) represents the kinetic reactions of three minerals. Reaction (R0) shows the equilibrium between CO₂ gas phase and dissolved phase and is only considered in the batch reaction modeling and is excluded in the subsequent reactive transport modeling due to no CO₂ free-gas phase considered in the latter.

2.1.1 Background batch reaction modeling

Background batch modeling is performed for adjusting the pressure and temperature as well as for dissolved species concentration and the related component species concentration in the domain. Initial vertical pressure in the domain is defined as hydrostatic pressure based on pressure gradient of 0.1 bar per meter below the earth surface [*Pruess, 2008*]. Vertical temperature distribution in the domain is based on the geothermal gradient of 0.03°C/m below the earth surface [*Pruess, 2008*]. Brinkman

equations are used in the background batch modeling for vertical pressure distribution in the domain thereby including the effects of acceleration due to gravity.

Initial concentration values of dissolved species and the related chemical components are obtained in the background batch reaction modeling by solving the geochemical system at CO₂ pressure (P_{CO_2}) of 0.01 bar assuming 0.5 M solution of sodium chloride while allowing the fluid-minerals geochemical interactions. Two cases of background batch modeling are performed; one assuming constant temperature of 27°C in the domain and the other one based on temperature gradient in the reservoir. All the involved geochemical reactions are defined as a function of temperature in the domain. In the batch reaction modeling, porosity of the reservoir as well as reactive surface area of minerals is assumed as constant.

2.1.2 CO₂ dissolution modeling

CO₂ dissolution modeling is performed to obtain CO₂-saturated brine composition and the related values of chemical component species required as boundary values in the injection stage. CO₂ dissolution modeling is performed at a temperature of 27 °C and pressure of 4.1 MPa for 0.5 M solution of sodium chloride. These temperature and pressure values correspond to the depth of the upper boundary of the modeled reservoir domain. CO₂ pressure is increased from background pressure of 0.01 bar to 41 bar as a function of time assuming that the CO₂ can be dissolved in the fluid within seconds (here 15s). CO₂ dissolution modeling is performed in the brine without including any mineral reactions.

2.2 Reactive transport modeling

2.2.1 Conceptual transport model

The domain used for CO₂-saturated brine injection consists of 250 m vertically thick and 1000 m wide [Figure 1]. 2D axisymmetric model is used in the transport modeling. In 2D axisymmetric model, the Cylindrical coordinates (r , z) replace the Cartesian coordinates (x , z) used in 2D geometry. 2D axisymmetric model represent 3D model with the assumption that no variations in any variable exists around the axis of revolution. Thus the use of 2D axisymmetric model instead of 3D, can reduce the computational burden significantly. For upper boundary of the reservoir ($z = 0$) considered lying at 400 m below the land surface, the lower boundary ($z = -250$ m) is at 650 m below the land surface.

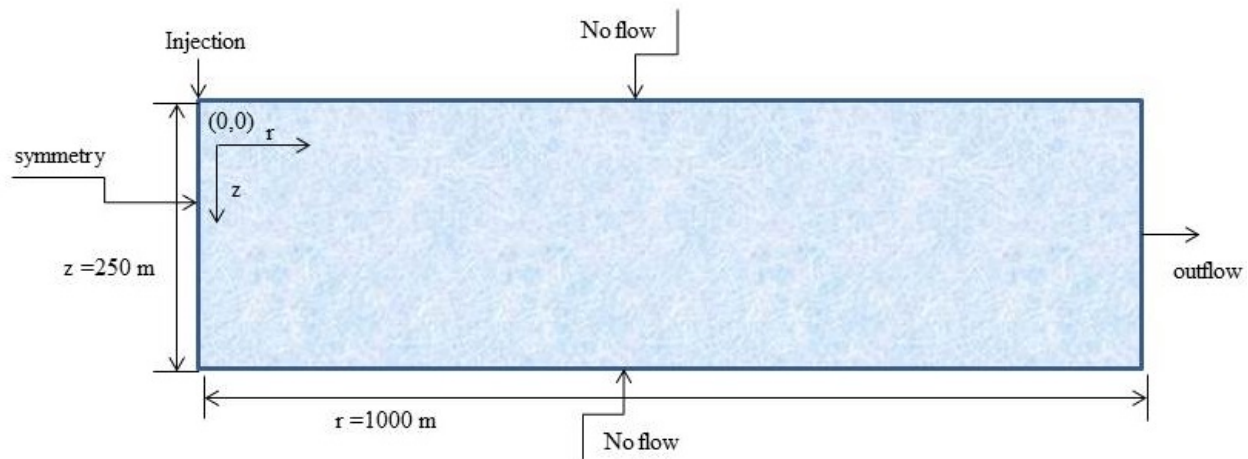


Figure 1. Schematic of subsurface geological reservoir for CO₂-saturated brine injection

Injection of CO₂-saturated brine is performed through a 0.1 m wide inlet boundary at the left-side ($0 \leq r \leq 0.1$) of the top boundary of the reservoir domain. CO₂-charged brine is injected in the reservoir at a constant rate of about 24 (kg/s) equivalently 0.95 (kg/s) of dissolved CO₂ for a period of 20 years. Symmetry condition exists at left vertical boundary ($r = 0$ m). Outflow of fluid takes place through the right vertical open boundaries ($r = 1000$ m) whereas no-flow conditions are applied at top and bottom

boundaries. The composition of carbonate reservoir minerals is taken from Zerai, 2006. The volume fraction of minerals is calculated from their respective weight percent assuming porosity of 25% (Table 2). This assumed porosity value of a carbonate reservoir lying at a depth of 400 m is based on the values reported by Al-Awadi et al., 2009.

Table 2. Composition of minerals for a carbonate reservoir opted from Zerai, 2006

Minerals	Weight percent	Volume fraction in solid mass	Volume fraction for a porosity of 25%
calcite	39	0.40	0.30
dolomite	60	0.59	0.44
siderite	1	6.95×10^{-3}	5.21×10^{-3}

2.2.2 Reactive transport formulation

In this reactive transport formulation we have considered the dissolved species as mobile whereas minerals are considered as immobile. The following equation is used to define the reactive transport system for aqueous species (mobile ones) written in terms of component species (\mathbf{u}) [*COMSOL Multiphysics*]:

$$\mathbf{R}_f \theta \frac{\partial \mathbf{u}}{\partial t} + (1 - \mathbf{K}_d \rho_p) \mathbf{u} \frac{\partial \theta}{\partial t} - \nabla \cdot [(\mathbf{D}_D + \mathbf{D}_e) \nabla \mathbf{u}] + \nabla \cdot (\mathbf{v} \mathbf{u}) = \theta \mathbf{r}_{geo} \quad (1)$$

$$\mathbf{R}_f = 1 + \frac{\rho_{bulk}}{\theta} \mathbf{K}_d \quad (2)$$

where \mathbf{u} is the vector of concentration (mol/kg fluid) of six chemical components; \mathbf{R}_f is a diagonal matrix of retardation factors; θ is the spatially and temporally varying medium porosity; ρ_{bulk} is the bulk density (kg per m³ bulk volume) of the porous media that is a

function of porosity and particle density; ρ_p is the particle density (kg/m^3); \mathbf{K}_d is a diagonal matrix where the diagonal elements include the sorption partition coefficients corresponding to six chemical components (m^3/kg); \mathbf{D}_d is the dispersion tensor (m^2/s); \mathbf{D}_e is the effective diffusion (diagonal) tensor (m^2/s) that is function of porosity of the medium; \mathbf{v} is Darcy's velocity vector (m/s) updated in space and time and finally \mathbf{r}_{geo} is the reaction term for consumption or production of component species (mol/kg fluid/s). A total of six chemical components involved in transport equation (1) are written as a linear combination of thirteen aqueous species, participating in seven equilibrium and three mineral kinetic reactions, based on the methodology presented by Saaltink et al. 1998 [Appendix A]. The source/sink term (\mathbf{r}_{geo}) and the equations required for speciation are also presented in Appendix-A. This reaction term represents the combined effect of all equilibrium as well as mineral kinetic reactions considered in the modeling. Due to involved six chemical components in the transport equation, \mathbf{u} is a vector of size 6 and \mathbf{R}_f and \mathbf{K}_d are matrices of size 6×6 . The transport equation (1) is thus a nonlinear partial differential equation in which the variables θ , ρ_p , ρ_{bulk} as well as the matrices \mathbf{R}_f and \mathbf{K}_d and the vector \mathbf{r}_{geo} , are all nonlinear functions of the local concentration of chemical components (\mathbf{u}). In the simulations, the diffusion coefficient for all the transport components is taken equal to $3.44 \times 10^{-9} \text{ m}^2/\text{s}$ whereas dispersivity is taken equal to $0.1\zeta \text{ m}$, where ζ is dimension of the transport domain. The dispersivity value is increased from 1 m to the maximum value over time ($\min(1 + 3.15 \times 10^{-5}t, 0.1\zeta)$) to avoid higher mass inflows due to higher dispersivity values at the initial stage of the transport simulation.

Because the involved minerals are considered as immobile and did not appear in equation (1), this requires implementing additional mass conservation equations for these minerals. Therefore the mass conservation of the three involved minerals undergoing the kinetic reactions in the transport domain is modeled through the following three ordinary differential equations (ODEs);

$$\frac{\partial \mathbf{c}^m}{\partial t} = -\mathbf{r}_{kin}^m \quad (3)$$

where \mathbf{c}^m is a vector of size 3 representing the concentration (mol/kg of fluid) of three minerals calcite, dolomite and siderite. The initial values of mineral concentrations are calculated from their respective initial volume fraction in the porous reservoir for an initial reservoir porosity of 0.25. The reaction term (\mathbf{r}_{kin}^m) is a vector of size 3 representing the kinetic reactions of three minerals. Mineral kinetic reactions are defined in terms of rate constant, concentration of aqueous species involved and the reactive surface area of the respective mineral [Lasaga et al., 1994]:

$$r_{kin}^m = k^m A^m [1 - \Omega^m] \quad (4)$$

where k^m is the temperature-dependent kinetic rate constant of the mineral (mol/m²/s), A^m is the mineral reactive surface area (m²/kg of fluid) updated in time and space, and the term $\Omega^m = Q^m / K_{eq}^m$ is saturation state of the respective mineral with K_{eq}^m as the equilibrium constant of mineral that is modeled as a function of temperature and Q^m as the ion activity product of the mineral. The temperature dependence of kinetic rate constant (k^m) of minerals is described by the Arrhenius equation [Lasaga, 1984]:

$$k^m = k_{25}^m \exp\left[-\frac{E_a^m}{R}\left(\frac{1}{T} - \frac{1}{298.15}\right)\right] \quad (5)$$

where R is the gas constant taken equal to 8.314 J/mol/K, T is temperature in K, E_a^m is the activation energy of the mineral and k_{25}^m is the reaction constant of mineral at 25 °C. The parameters and initial value of variables used in equations (3) through (5) for minerals calcite, dolomite, and siderite are presented in Table 3.

Table 3. Parameters and initial values of variables used in equations (3)-(5) for minerals calcite, dolomite, and siderite

Mineral	k_{25}^m * (mol/m ² /s)	E_a^m * (KJ/mol)	A^{m**} (m ² /kg fluid)	c^{m**} (mol/kg fluid)
calcite	1.60×10 ⁻⁹	41.87	21.80	32.47
dolomite	0.6×10 ⁻⁹	41.87	31.73	27.11
siderite	0.6×10 ⁻⁹	41.87	0.37	0.72

*Opted from Xu et al., 2004

**Initial values are calculated from initial volume fraction (corresponding to reservoir porosity of 0.25) of minerals in porous rock formation

Over the period of time minerals dissolution or precipitation causes changes in concentration of minerals (through equation (3)) that in turn changes the minerals volume fraction and porosity of the porous media. The variations in porosity of the porous media are modeled as a function of variations in volume fractions of the minerals in the porous media [TOUGHREACT]:

$$\theta = 1 - \sum_{m=1}^n VF_p^m \quad (6)$$

where n is the number of minerals forming the porous rock media and the term $VF_p^m = V_p^m / V_p^{rock}$ (m^3 of mineral/ m^3 of porous rock medium) is the volume fraction of the mineral expressed as the ratio of the mineral volume to the total volume of porous rock including porosity. It is important to mention here that none of the minerals is allowed to completely dissolve and disappear from the transport domain. Medium porosity is also kept below unity by setting a minimum threshold concentration value of all involved minerals equal to 1×10^{-13} (mol/kg fluid) in equation (3) [TOUGHREACT]. Also in this study the porosity of the medium is not allowed to go below a minimum value of 0.001 by stopping any further minerals precipitation whenever the porosity reaches this minimum value.

Brinkman equations are used to describe the velocity field (\mathbf{v}) in the reactive transport system (1). Brinkman equations combine the continuity equation with the momentum balance equation to define the flow in porous media:

$$\frac{\partial}{\partial t}(\theta \rho_b) + \nabla \cdot (\rho_b \mathbf{v}) = Q \quad (7)$$

$$\frac{\rho_b}{\theta} \left[\frac{\partial \mathbf{v}}{\partial t} + (\mathbf{v} \cdot \nabla) \frac{\mathbf{v}}{\theta} \right] = -\nabla p + \nabla \cdot \left\{ \frac{\mu_b}{\theta} \left[(\nabla \mathbf{v} + (\nabla \mathbf{v})^T) - \frac{2}{3} (\nabla \cdot \mathbf{v}) \mathbf{I} \right] \right\} - \left(\frac{\mu_b}{\kappa} + \frac{Q}{\theta^2} \right) \mathbf{v} + \mathbf{F} \quad (8)$$

where ρ_b is the density (kg/m^3) and μ_b is the dynamic viscosity ($\text{kg}/\text{m}/\text{s}$) of CO_2 -saturated NaCl brine, p is the pressure (Pa), κ is the permeability of the porous medium (m^2), and Q is the mass source or sink, which is taken as zero in this study. Gravitational influence is accounted

through the force term ($\mathbf{F} = -\rho_b \mathbf{g}$) with \mathbf{g} as gravitational acceleration vector (9.81 m/s²). The density and viscosity of brine are calculated as a function of temperature, pressure and dissolved species (Na⁺, Cl⁻, and CO_{2aq}). However, in this study the values of temperature and pressure are based on constant vertical gradients in the reservoir for calculation of brine density and viscosity. The equations related to CO₂-saturated brine density, viscosity, updating the medium porosity and the reactive surface area of involved minerals have been presented by *Ahmad et al.*, 2014 (a,b). Here these equations are provided in the form of supplementary information for ready reference. Variation in permeability of the medium is modeled in relation to the variations in porosity and specific surface area of rock using the Kozeny-Carman relation [*Bear and Cheng*, 2010]:

$$k = C_0 \frac{\theta^3}{(1-\theta)^2 \left(A_{SSAV}^{rock} \right)^2} \quad (9)$$

where C_0 is taken equal to 0.2 [*Bear and Cheng*, 2010] and A_{SSAV}^{rock} is specific surface area of the solid rock per unit volume of solid rock updated in time and space. For the considered combination of initial porosity (0.25) and initial minerals volume fraction we found an initial permeability as $6.460 \times 10^{-13} \text{ m}^2$ for the reservoir.

2.2.3 Heat transfer

The temperature of the injected CO₂-saturated brine injection can be expected to be relatively lower than the prevailing temperature in the reservoir. The example may be the heat recovery from the hotter brine, either for power production or heating purposes, pumped out of the reservoir and its injection back in the reservoir after saturated with dissolved CO₂ [CO₂-

DISSOLVED]. However, in this study brine carrying dissolved CO₂ was injected at a temperature of 27°C (represents the temperature conditions of the upper boundary of the reservoir). Thus the injected brine may shift the cooling effects through thermal exchanges with the resident brine and the porous media in the reservoir. The resulting cooling in the reservoir may affect the geochemical reactions defined as a function of temperature. Heat-exchange between the injected CO₂-saturated brine and the porous media of the reservoir is modeled using the following heat transfer equation [*COMSOL Multiphysics*]:

$$\left(\rho C_p\right)_{eq} \frac{\partial T}{\partial t} + \rho_b C_{p,b} \mathbf{v} \cdot \nabla T = \nabla \cdot \left(k_{eq} \nabla T\right) + \nabla \cdot k_d \nabla T \quad (10)$$

where

$$\left(\rho C_p\right)_{eq} = (1 - \theta) \rho_{pm} C_{p,pm} + \theta \rho_b C_{p,b} \quad (11)$$

and

$$k_{eq} = (1 - \theta) k_{pm} + \theta k_b \quad (12)$$

Where $\left(\rho C_p\right)_{eq}$ is the volume averaged heat capacity at constant pressure of the fluid and the porous media, k_{eq} is the volume averaged thermal conductivity of fluid and the porous media, \mathbf{v} is the fluid velocity representing the Darcy velocity defined through Brinkman equations, k_d is the thermal dispersion taken equal to 1 m, ρ_{pm} is density of the porous medium, $C_{p,pm}$ is heat capacity of the porous media, $C_{p,b}$ is heat capacity of the fluid, k_{pm} is thermal conductivity of porous media and k_b is thermal conductivity of the brine fluid. Thermal conductivity for porous media (k_{pm}) is taken equal to 2.51 W/m/K and

specific heat capacity of rock ($C_{p,pm}$) is taken equal to 920 J/kg/K [Pruess, 2005]. The relations for heat capacity and thermal conductivity of CO₂-saturate brine are presented in Appendix-B.

2.2.4 Various transport simulation scenarios

Four scenarios of reactive transport modeling are performed for a period of 20 years [Table 4]. Sorption of species on the minerals surfaces was included only in scenario 4. Scenario 1 is performed at a constant temperature of 27°C in the reservoir (T constant). In scenario 2, temperature in the reservoir is based on constant geothermal gradient (T gradient). In scenarios 3 and 4, heat transfer between the injected CO₂-saturated brine and the porous media of the reservoir is also included in the transport analysis (T flow). These simulation scenarios are performed to analyze the effects of constant temperature in reservoir, temperature gradient in the reservoir, and the heat transfer included in the modeling on the mass uptake of CO₂ in geochemical reactions. In all these scenarios geochemical reactions (equilibrium as well as mineral kinetic) are defined as a function of temperature. However, brine density and viscosity are modeled as a function of P and T gradients in order to obtain similar values of density and viscosity and to eliminate the effects on the results due to differences in density and viscosity between these scenarios. In addition to these four reactive transport scenarios, four equivalent mass transport scenarios are also performed where no geochemical reactions those presented in Table 1 are included. The comparison of mass balance between the transport scenario and the corresponding reactive transport scenarios gives an accurate value of uptake of CO₂ in geochemical reactions. The uptake of CO₂ in geochemical reactions is calculated based on cumulative quantities of CO₂ mass injected in the reservoir, mass stored in the

aqueous state, and the mass leaving the transport domain through the outlet boundary over the considered period of time.

Table 4. Various reactive transport simulation scenarios

Scenarios	Sorption	T conditions in the reservoir
1	No	T constant
2	No	T gradient
3	No	T flow
4	Yes	T flow

2.2.5 Initial and boundary conditions

The initial values of pressure, temperature, concentration of dissolved species and related component species are obtained from background batch reaction modeling. The boundary values of component species representing the composition of CO₂-saturated brine to be injected were obtained from CO₂ dissolution modeling. Initial and boundary values of species are defined in terms of chemical components since the transport takes place in terms of chemical components. COMSOL Multiphysics make it possible to save the previous numerical solution from the background batch reaction modeling and use it as initial conditions in the subsequent transport modeling. Opted this strategy requires only defining the boundary values of species concentration in terms of chemical components [Table 5]. These chemical components represent the composition of CO₂-saturated brine obtained from CO₂-dissolution modeling (Table 7).

Table 5. Boundary conditions (sub-index *bc*) in terms of chemical components

Chemical component*	Concentration (mol/kg brine)
${}^u\text{HCO}_3{}_{bc}$	5.977×10^{-3}

$u_{Na_{bc}}$	0.5
$u_{Ca_{bc}}$	2.698×10^{-3}
$u_{Mg_{bc}}$	2.585×10^{-4}
$u_{Fe_{bc}}$	3.091×10^{-5}
$u_{CO2_{bc}}$	0.902

* u represents the chemical component

3 Results and discussion

3.1 Background batch reaction modeling and resident brine composition

For vertical extent of 250 m with upper boundary supposed at 400 m below the land surface we obtain a value of 4.1 MPa at the top and 6.6 MPa at bottom of the domain. For a fixed temperature of upper boundary at 27 °C we achieve a temperature of 34.5 at bottom of the reservoir.

Table 6 presents the composition of resident brine in the reservoir, obtained from the background batch reaction modeling for the case of temperature gradient considered in the reservoir. The solution equilibrates at pH values of 7.26 and 7.27 at top and bottom of the reservoir respectively. Column 2 of Table 6 also represents the brine composition for the background batch reaction modeling performed while assuming constant temperature of 27 °C in the reservoir. At a pressure of 0.01 bar, dissolution and precipitation of involved minerals is found negligible, that provides a justification of assuming constant mineral reactive surface area as well as constant porosity and permeability of the reservoir in the background batch reaction modeling. Geochemical conditions obtained from

background batch reaction modeling are in equilibrium with respect to all the minerals involved.

Table 6. Composition of resident brine in the reservoir obtained from background batch reaction modeling for the case of temperature gradient in the reservoir

Species	concentration (mol/kg) (top boundary of the reservoir)	concentration (mol/kg) (lower boundary of the reservoir)
CO _{2aq}	2.885×10 ⁻⁴	2.435×10 ⁻⁴
HCO ₃ ⁻	4.637×10 ⁻³	4.078×10 ⁻³
Na ⁺	0.499	0.499
Cl ⁻	0.500	0.500
H ⁺	5.506×10 ⁻⁸	5.365×10 ⁻⁸
OH ⁻	4.063×10 ⁻⁷	6.719×10 ⁻⁷
CO ₃ ²⁻	1.680×10 ⁻⁵	1.614×10 ⁻⁵
NaHCO _{3aq}	1.248×10 ⁻³	9.679×10 ⁻⁴
Ca ²⁺	2.645×10 ⁻³	2.290×10 ⁻³
Mg ²⁺	2.546×10 ⁻⁴	2.014×10 ⁻⁴
Fe ²⁺	3.022×10 ⁻⁵	2.445×10 ⁻⁵
CaHCO ₃ ⁺	5.312×10 ⁻⁵	4.342×10 ⁻⁵
MgHCO ₃ ⁺	3.941×10 ⁻⁶	2.894×10 ⁻⁶
FeHCO ₃ ⁺	6.870×10 ⁻⁷	4.277×10 ⁻⁷

3.2 Solubility of CO₂ and composition of resulting CO₂-saturated brine

CO₂ solubility modeling is performed at the pressure and temperature conditions representative of upper boundary of the reservoir. In the solubility modeling, CO₂ was made dissolved in the resident brine of composition given in column 2 of Table 6 that is supposed to be pumped out of the targeted subsurface reservoir. Table 7 shows the

composition of CO₂-saturated brine, obtained from solubility modeling, to be injected in the geological reservoir. Concentration of dissolved CO₂ in the resulting CO₂-saturated brine increases from a value of 2.885×10⁻⁴ mol/kg to a value of 0.902 mol/kg. Increased concentration of dissolved CO₂ resulted in a decrease in pH of brine from 7.26 to a value of 3.78. According to the solubility modeling performed at temperature of 27°C and pressure of 41 bar (conditions representing the depth of 400 m below the land surface), about 25.2 kg mass of brine fluid will be needed to dissolve one kg of CO₂.

Table 7. Composition of CO₂-saturated brine obtained from CO₂-dissolution modeling

Species	concentration (mol/kg)
CO _{2aq}	0.902
HCO ₃ ⁻	4.794×10 ⁻³
Na ⁺	0.499
Cl ⁻	0.5
H ⁺	1.665×10 ⁻⁴
OH ⁻	1.344×10 ⁻¹⁰
CO ₃ ²⁻	5.740×10 ⁻⁹
NaHCO _{3aq}	1.290×10 ⁻³
Ca ²⁺	2.644×10 ⁻³
Mg ²⁺	2.544×10 ⁻⁴
Fe ²⁺	3.020×10 ⁻⁵
CaHCO ₃ ⁺	5.487×10 ⁻⁵
MgHCO ₃ ⁺	4.072×10 ⁻⁶
FeHCO ₃ ⁺	7.095×10 ⁻⁷

The saturation state of resulting CO₂-saturated brine fall well below unity and thus below equilibrium with respect to the minerals involved [Table 8]. The lower saturation state of CO₂-saturated brine to be injected with respect to the minerals involved may cause successive dissolution of the minerals particularly near the injection point in the reservoir during the injection process.

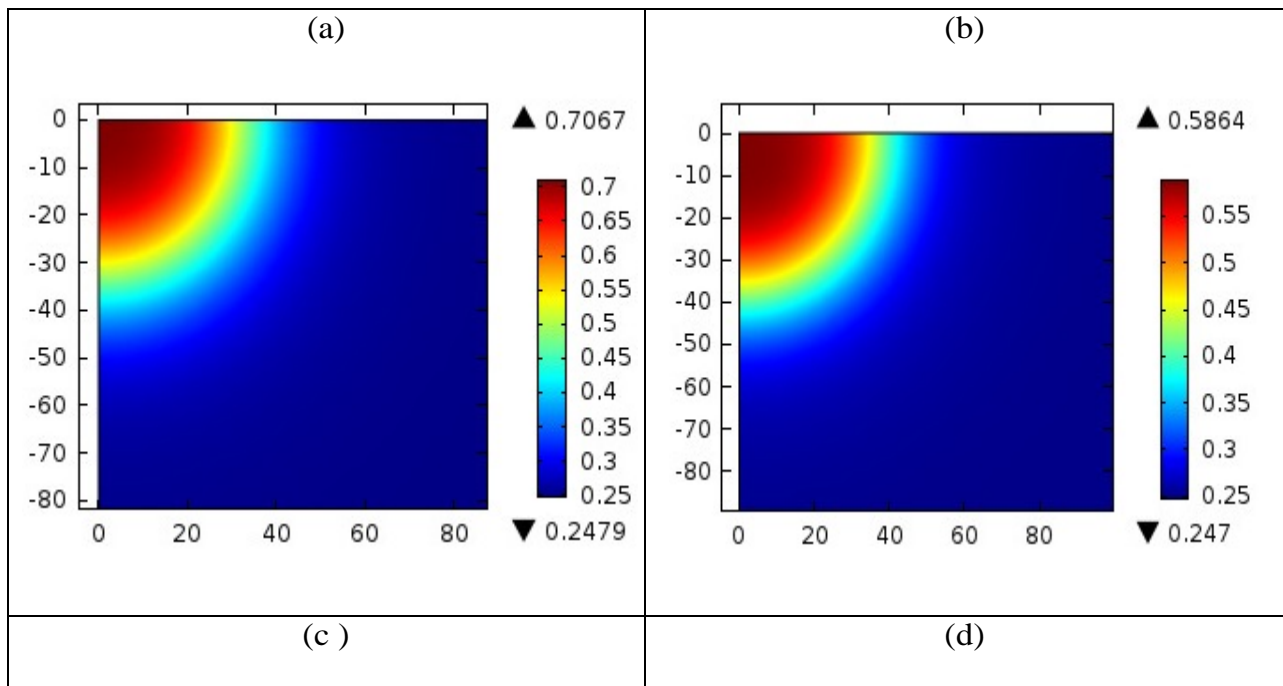
Table 8. Saturation state of CO₂-saturated brine with respect to minerals considered

Mineral	Saturation state of CO ₂ -saturated brine with respect to minerals
calcite	3.426×10^{-4}
dolomite	1.167×10^{-7}
siderite	3.415×10^{-4}

3.3. Reactive transport

Injected brine saturated with CO₂ is not only low in pH but also under-saturating conditions with respect to the considered minerals calcite, dolomite and siderite. Geochemical interactions of injected brine with the reservoir minerals have initiated minerals dissolution reaction in the vicinity of the injection point. The reaction zone advances with the lateral and downward movement of CO₂-saturated brine in the reservoir. Dissolution of minerals calcite, dolomite, and siderite caused by injected low pH CO₂-saturated brine results in the consumption of CO₂. However, precipitation of these minerals may release CO₂ back into the brine. In the reactive transport modeling these minerals were allowed either to dissolve or precipitate in the reservoir driven by injected CO₂-saturated brine. Dissolution and precipitation of minerals has resulted in variations in porosity with associated changes in permeability of the media and also the minerals reactive surface area. Significant changes in porosity have been observed in the vicinity of the

injection point extending up to about 45 m in the reservoir. Figure 2 shows the porosity variations in various reactive transport scenarios after 20 years of simulation time. Higher minerals dissolution in scenario 1 has resulted in higher porosity value as compared to the rest of the scenarios. In scenario 1 the values of porosity reached to a value of 0.71 from its initial value of 0.25. Variations in permeability were also observed as linked to the porosity. In scenario 1, medium permeability has attained a value of $6.54\text{E-}11 \text{ m}^2$ from an initial value of $6.46\text{E-}13 \text{ m}^2$.



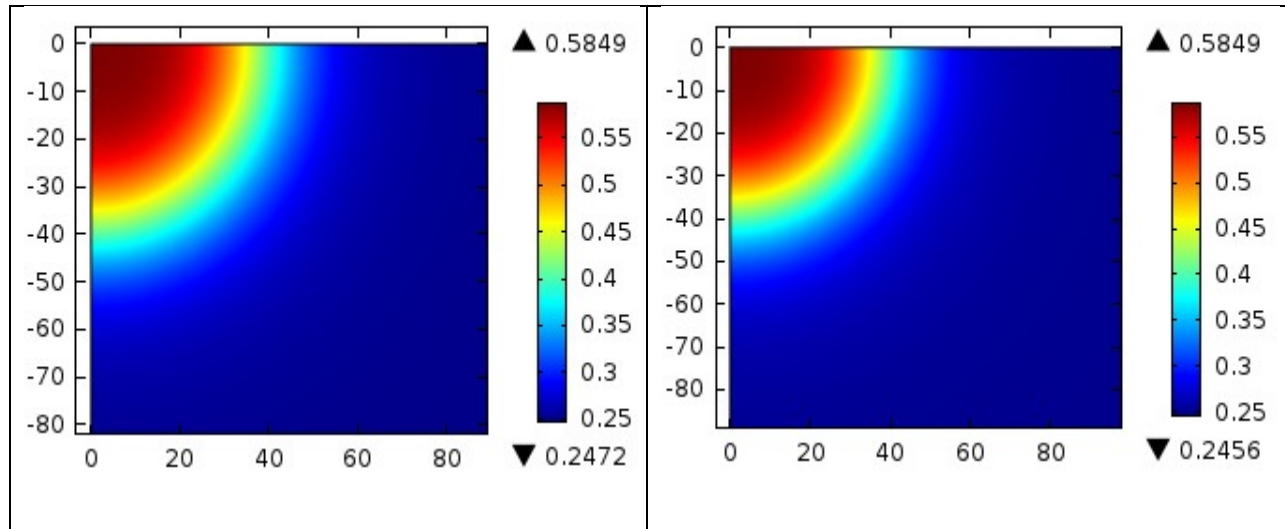


Figure 2. Variations in medium porosity in various reactive transport scenarios from initial porosity value of 0.25; scenario 1 (a), scenario 2 (b), scenario 3 (c) and scenario 4 (d)

Higher minerals dissolution compared to their respective precipitation in the reservoir has resulted in net uptake of CO₂ due to geochemical reactions in the reservoir. With only minor differences, all the reactive transport scenarios have resulted in almost same uptake of CO₂ mass in geochemical reactions. Figure 3 presents the percentage mass consumption of CO₂ due to combined effect of equilibrium and minerals kinetic reactions over a simulation period of 20 years. Scenario-1 (T constant) has shown the highest mass uptake of CO₂ followed by scenario 4 (T flow and including sorption), scenario 3 (T flow) and then scenario 2 (T gradient). Almost a constant rate of CO₂ mass uptake of around 18% was observed after 5 years in all the reactive transport scenarios.

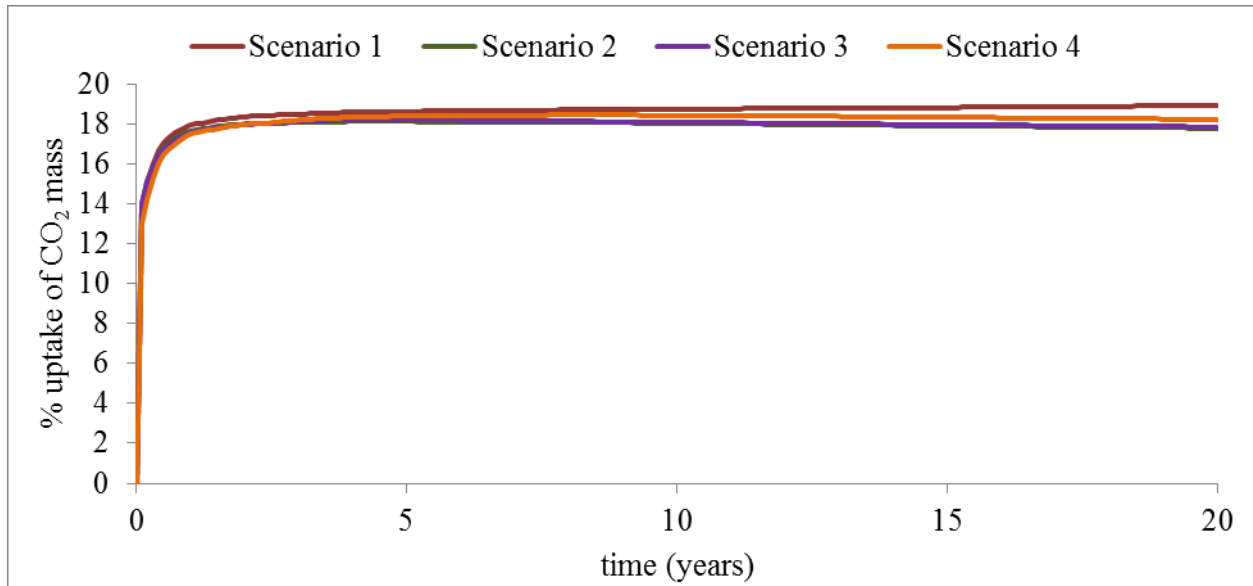


Figure 3. Percent mass uptake of CO₂ due to geochemical reactions in various reactive transport scenarios

Table 9 presents the mass balance of dissolved CO₂ in the reservoir after simulation time of 20 years. The total mass uptake of CO₂ (tonnes) is highest in scenario 4 followed by scenario 1, scenario 3 and scenario 2. However, the percent rates of mass uptake were found as 18.219%, 18.917%, 17.845% and 17.778% in scenario 4, scenario 1, scenario 3 and scenario 2 respectively. Although higher cumulative mass uptake resulted in scenario 4 compared to scenario 1 but the calculated rates of mass uptake is lower in scenario 4 compared to the corresponding rate in scenario 1. This lower rate of mass uptake in scenario 4 compared to scenario 1 is due to the fact that the percent rates of mass uptake are calculated in relation to the cumulative mass inflows. Higher mass uptake in geochemical reactions has caused relatively higher mass inflows through the injection boundary mainly due to increased dispersive flux and to the lesser extent due to diffusive flux. From Table 9, we can see that the cumulative quantities of mass inflows have direct relationship with the cumulative quantities of mass uptake in geochemical reactions.

Higher consumption and uptake of CO₂ in geochemical reactions has caused a decrease in total mass stored in aqueous state. Sorption process that was included in scenario 4, has also resulted in higher mass uptake of CO₂ in geochemical reactions compared to the corresponding scenario 3 where no sorption was included in the transport analysis. In scenario 4 we observe that the quantity of dissolved CO₂ injected in the reservoir was partitioned between the aqueous phase (50.01%) and the adsorbed state (34.77%). It can also be seen that only very small quantities of CO₂ have left the reservoir through the outflow boundary on the right hand side of the simulation domain over the period of 20 years.

Table 9. Mass (tonnes) balance of CO₂ in various reactive transport scenarios after 20 years of simulation time

Scenarios	Scenario 1	Scenario 2	Scenario 3	Scenario 4
Mass injected in the reservoir	7.224E+05	7.156E+05	7.156E+05	7.702E+05
Mass stored in aqueous state	6.058E+05	6.085E+05	6.080E+05	3.692E+05
Mass stored in sorbed state	0.000E+00	0.000E+00	0.000E+00	2.567E+05
Mass uptake in geochemical reactions	1.367E+05	1.272E+05	1.277E+05	1.651E+05
% mass uptake in geochemical reactions at time of 20 years	18.917	17.778	17.845	21.442
Mass left the domain	1.822E+02	1.647E+02	1.653E+02	1.658E+02

Minerals dissolution and precipitation in the reservoir has caused to change the porosity and thus the total pore space of the reservoir. Table 10 presents the total void spaces in the reservoir in various reactive transport scenarios at the end of 20 years of simulation time. Comparing the

reactive transport scenarios, it can be observed that higher quantities of CO₂ mass uptake due to geochemical reactions (Table 9) has resulted in higher total pore spaces in the reservoir (Table 10).

Table 10. Variations in total pore spaces in the reservoir at time of 20 years in various reactive transport scenarios

Scenarios	Scenario 1	Scenario 2	Scenario 3	Scenario 4
initial	1.96350E+08	1.96350E+08	1.96350E+08	1.96350E+08
Final	1.96437E+08	1.96434E+08	1.96435E+08	1.96439E+08
% increase	4.43086E-02	4.27807E-02	4.32900E-02	4.53272E-02

4. Discussions

As a result of solubility of CO₂ in the NaCl brine, pH was dropped down to a value of 3.78 from its initial value of 7.26 in the resident brine. CO₂ was dissolved in the brine in the absence of any geochemical interactions with the minerals. This significant drop in pH was mainly due to the absence of any buffer to the solution which is otherwise provided by the carbonate minerals in the subsurface. This pH value can be expected value in the absence of carbonate minerals [Lagneau, et al., 2005; Hellevang, 2006; Pokrovsky et al. 2009; Gaus, 2010]. Thus dissolution of CO₂ in the brine has made the resulting CO₂-saturated brine more acidic with high geochemical reactivity.

Reaction stoichiometry of minerals calcite, and siderite shows that one mole of H⁺ is consumed while one mole of each of Ca²⁺, and Fe²⁺ ions is produced in dissolution of respective minerals. However, dissolution of mineral dolomite is associated with consumption of two moles of H⁺ from the solution while producing one mole of each Ca²⁺ and Mg²⁺ ions in the solution. This consumption of H⁺ associated with minerals dissolution results in consumption of dissolved

CO₂[Dreybrodt et al., 1996; Kaufmann and Dreybrodt, 2007]. However, precipitation of these minerals is associated with production of H⁺ with associated release of CO₂ in the brine solution [Dreybrodt et al., 1997]. Net uptake of CO₂ in geochemical reactions has thus resulted due to higher dissolution of minerals compared to their respective precipitation in the reservoir driven by low pH CO₂-saturated brine.

Higher CO₂ uptake in scenario 1 compared to the scenarios 2 and 3 has been due to considered constant temperature in the reservoir. A constant temperature of 27°C considered in the reservoir increased the value of equilibrium constants of reactions of considered minerals as compared to the values of equilibrium constants in scenarios 2, and 3 where temperature was increased with depth due to temperature gradient considered in the reservoir. Relatively lower values of equilibrium constants in scenarios 2 and 3 caused a decrease in dissolution of the considered minerals resulting in lower quantities of mass uptake of CO₂ in geochemical reactions as compared to the mass uptake of CO₂ in scenario 1. Resulting higher minerals dissolution in scenario 1 has also caused higher porosity and permeability in the reservoir than the corresponding values observed in scenarios 2 and 3 (Figure 2). Higher mass uptake in scenario 4 compared to the corresponding scenario 3 has been due to the sorption included in the transport analysis. Sorption has also resulted in significant additional quantities of CO₂ stored in the adsorbed state in the reservoir (Table 9). The quantities of adsorbed state mass of CO₂ in the reservoir, however depends on the value of sorption partition coefficient.

Comparing the porosity variations (Figure 2) and the values of CO₂ mass uptake (Table 9) we see that these variables are loosely related to each other. In scenarios 1 and 2 we can observe that higher minerals dissolution with higher mass uptake of CO₂ has resulted in higher medium porosity. However this relationship does not exist in scenario 2 Vs scenario 3 and scenario 3 Vs

scenario 4. In scenario 3 the mass uptake of CO₂ is higher as compared to the uptake in scenario 2 but the maximum value of porosity is lower in scenario 3 than in scenario 2. Similarly higher mass uptake of CO₂ exists in scenario 4 as compared to scenario 3 but the maximum porosity value is same in both these scenarios. Thus the variations in porosity, permeability and reactive surface area is a complex function of spatial distribution of minerals dissolution and precipitation of all the minerals involved as well as of the sorption when included in the transport analysis. However, comparing the various reactive transport scenarios it was observed that increase in total pore space of the reservoir (Table 10) has direct relationship with the quantities of mass uptake of CO₂ in geochemical reactions (Table 9). It was also observed that in all the reactive transport scenarios none of the minerals was completely dissolved.

4. Conclusions

In this study we have explored a relatively safer way of CO₂ geological storage in shallow carbonate reservoir. Injection of CO₂-saturated brine has been performed in the subsurface hypothetical carbonate reservoir at a depth of 400 m below the land surface. Injected brine saturated with CO₂ being low in pH and in under-saturation conditions with respect to the considered minerals resulted in higher minerals reactivity with significant mass uptake of dissolved CO₂ through considered equilibrium and minerals kinetic reactions. Minerals dissolution has increased the pore spaces resulting in increased storage capacity for CO₂ in aqueous phase. Sorption of species on the mineral surfaces has provided the additional retention capacity for injected CO₂ in the reservoir.

This study has quantified the mass stored in aqueous state, mass stored in the adsorbed state and the amount of CO₂ converted into other ions (ionic trapping) in relation to the quantities of dissolved CO₂ injected in the reservoir. The storage of injected mass of dissolved CO₂ in the reservoir has been in the form of dissolved phase, ionic trapping and the mass stored in adsorbed state. However, the considered carbonate reservoir did not provide any significant permanent storage through minerals precipitation (mineral trapping) due to insignificant precipitation of minerals taken place in the reservoir.

Larger volumes of brine fluid may involve for injection of bulk quantities of dissolved CO₂ with associated higher costs involved. Although sorption has resulted in storage of additional quantities of CO₂, proper evaluation of sorption properties of minerals is very important for the quantification of CO₂ mass stored in adsorbed state in the reservoir.

Acknowledgements

This work was partly funded by Higher Education Commission (HEC) of Pakistan in the form of scholarship, Lars Erik Lundberg Scholarship Foundation, Sweden. Special thanks go to my employer, Ministry of Petroleum and Natural Resources, Government of Pakistan for granting me the study leave for this research work. Xavier Sanchez-Vila acknowledges support from the ICREA Academia program.